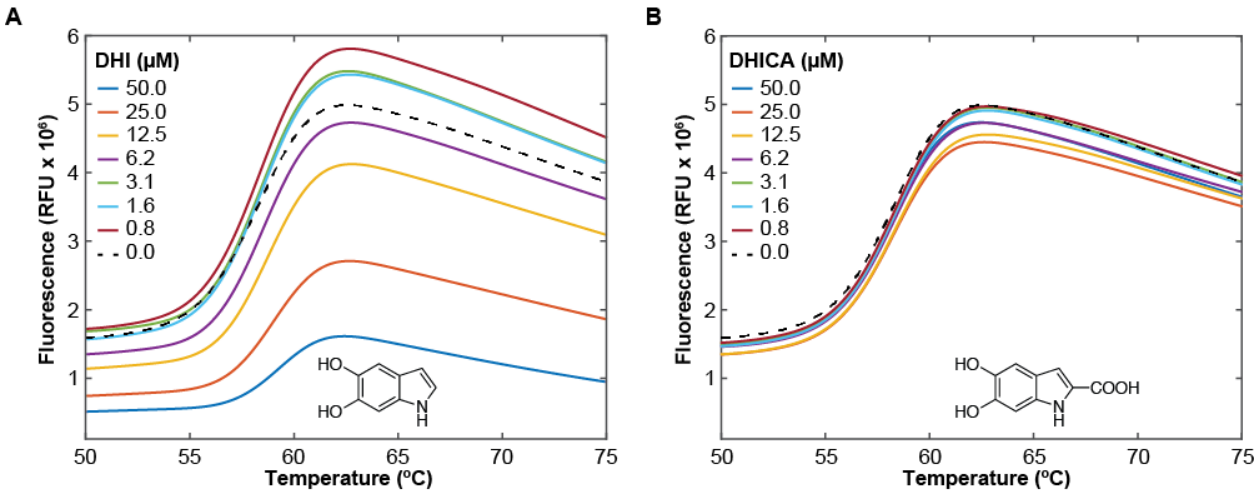

Figure S1. (Related to Figure 2) DHI but not DHICA decreases the overall SYPRO orange fluorescence. DSF assays were carried out on the Nurr1 LBD (4 μM) in the presence of the dye SYPRO orange (2.5x) and varying concentrations of DHI or DHICA. **(A, B)** Plot of the fluorescence (RFU) as a function of temperature for Nurr1 in the presence of increasing concentrations of (A) DHI and (B) DHICA. Experiments were performed in triplicate.

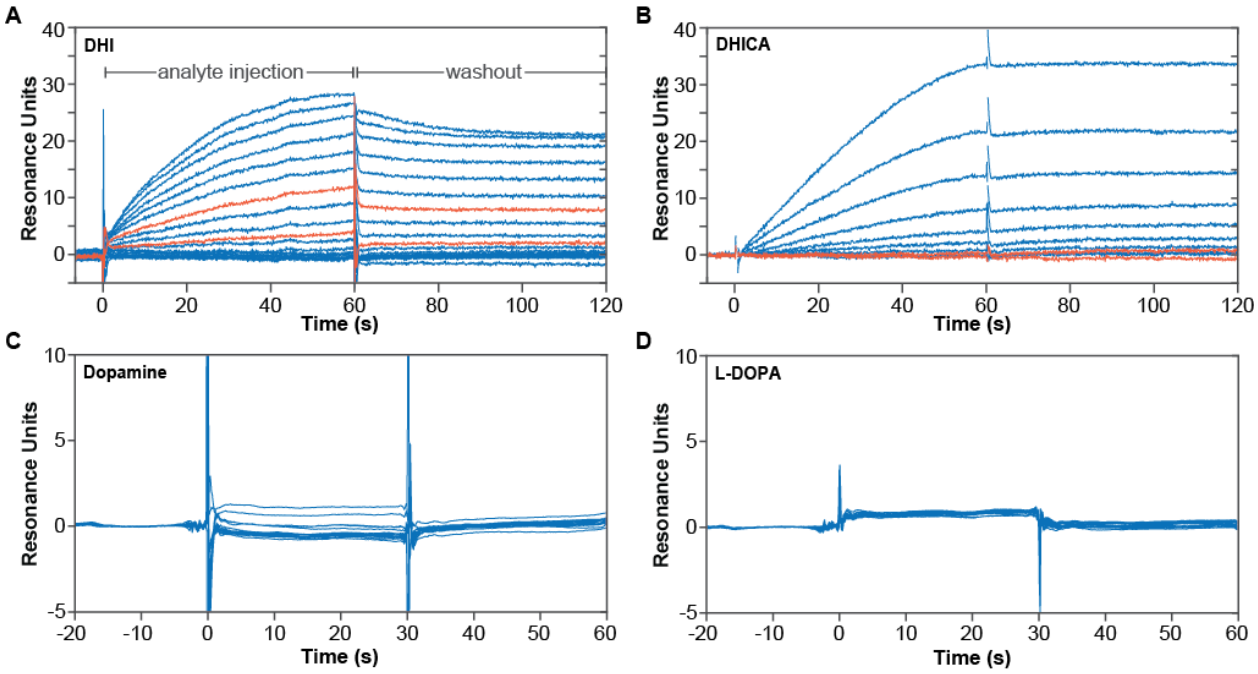

Figure S2. **(Related to Figure 3)** Specific association of DHI, but not DHICA, dopamine or L-DOPA, with the Nurr1 LBD measured by surface plasmon resonance. Biotinylated Nurr1 LBD was coupled to a streptaviden-coated biosensor chip and exposed to analytes at varying concentrations without surface regeneration between exposures. **(A)** Concentration-dependent association of DHI with Nurr1 LBD. DHI was injected at 15 increasing concentrations (16.8 μM DHI, 0.6x dilutions down to 0.01 μM; 60 s association time). Sensorgrams for DHI injections at 0.17 and 0.78 μM are highlighted in orange. **(B)** Non-specific association of DHICA with Nurr1 LBD. DHICA was injected at 11 increasing concentrations (25.9 μM DHICA, 0.6x dilutions down to 0.16 μM; 60 s association time). Sensorgrams for DHICA injections at 0.16 and 0.73 μM are highlighted in orange. **(C, D)** No association of dopamine or L-DOPA with Nurr1 LBD. Analytes were injected at 16 increasing concentrations (100 μM dopamine or L-DOPA, 0.6x dilutions down to 0.05 μM; 30 s association time).

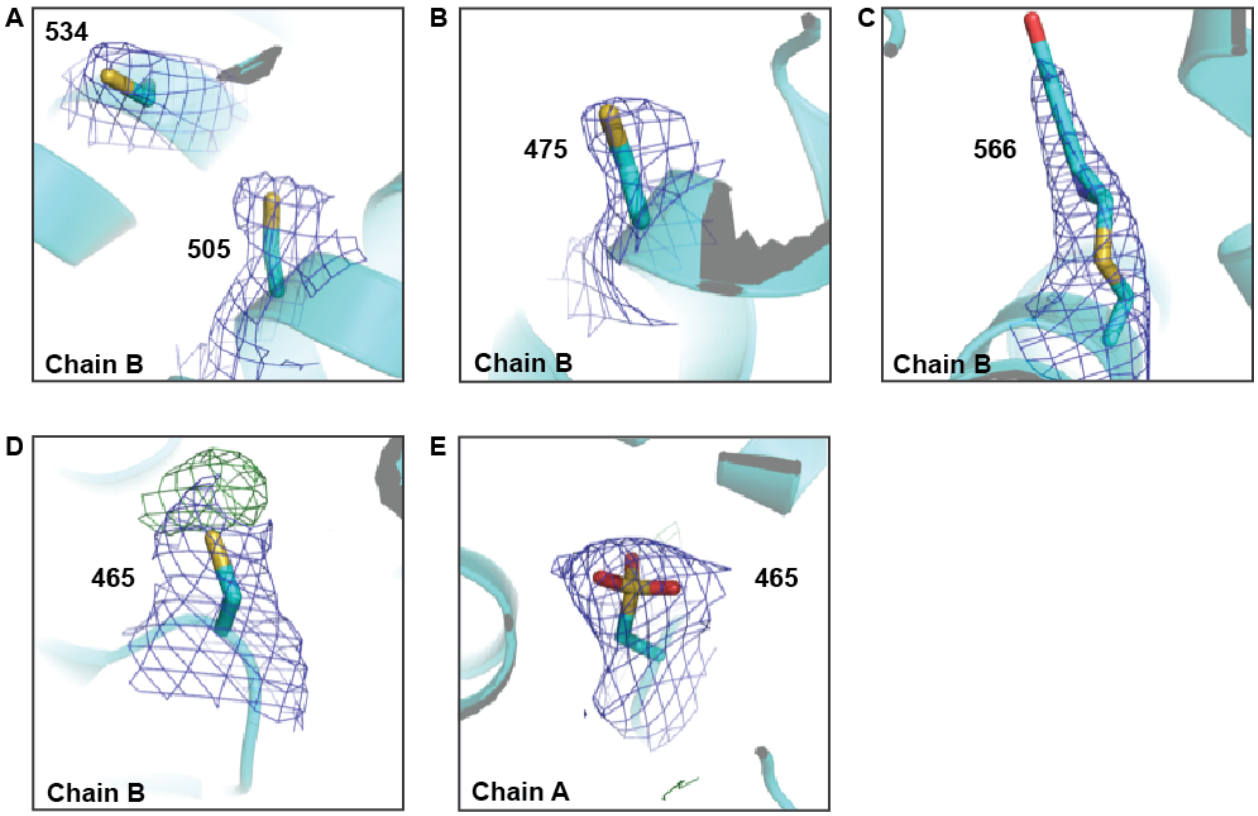

Figure S3. **(Related to Figure 4)** Electron density of all cysteine residues in the Nurr1 LBD-IQ structure. Electron density map (2mFo-DFc; contoured to 1σ) is shown in blue mesh. Difference density map (mFo-DFc; contoured to 3σ) is shown in green mesh. Cysteines 534, 505, and 475 show no positive density around their respective sulfur atoms in all three chains (data for Chain B shown), whereas Cys566 shows positive electron density around its sulfur atom that is consistent with the IQ-adduct in each chain. Cysteine 465 shows positive electron density around the sulfur atom in Chain B and Chain A. However, an IQ adduct at this position is precluded by severe steric clashes. Rather, the electron density is satisfied by modeling oxidized cysteine (sulfonic acid) at this position in Chain A (70% occupancy), but not Chain B, using occupancy refinement; accordingly, Cys465 of Chain B still shows positive electron density around its sulfur atom. Notably, Cys465 is near two arginine residues (Arg450 and Arg454) that could favorably interact with oxidized cysteine.

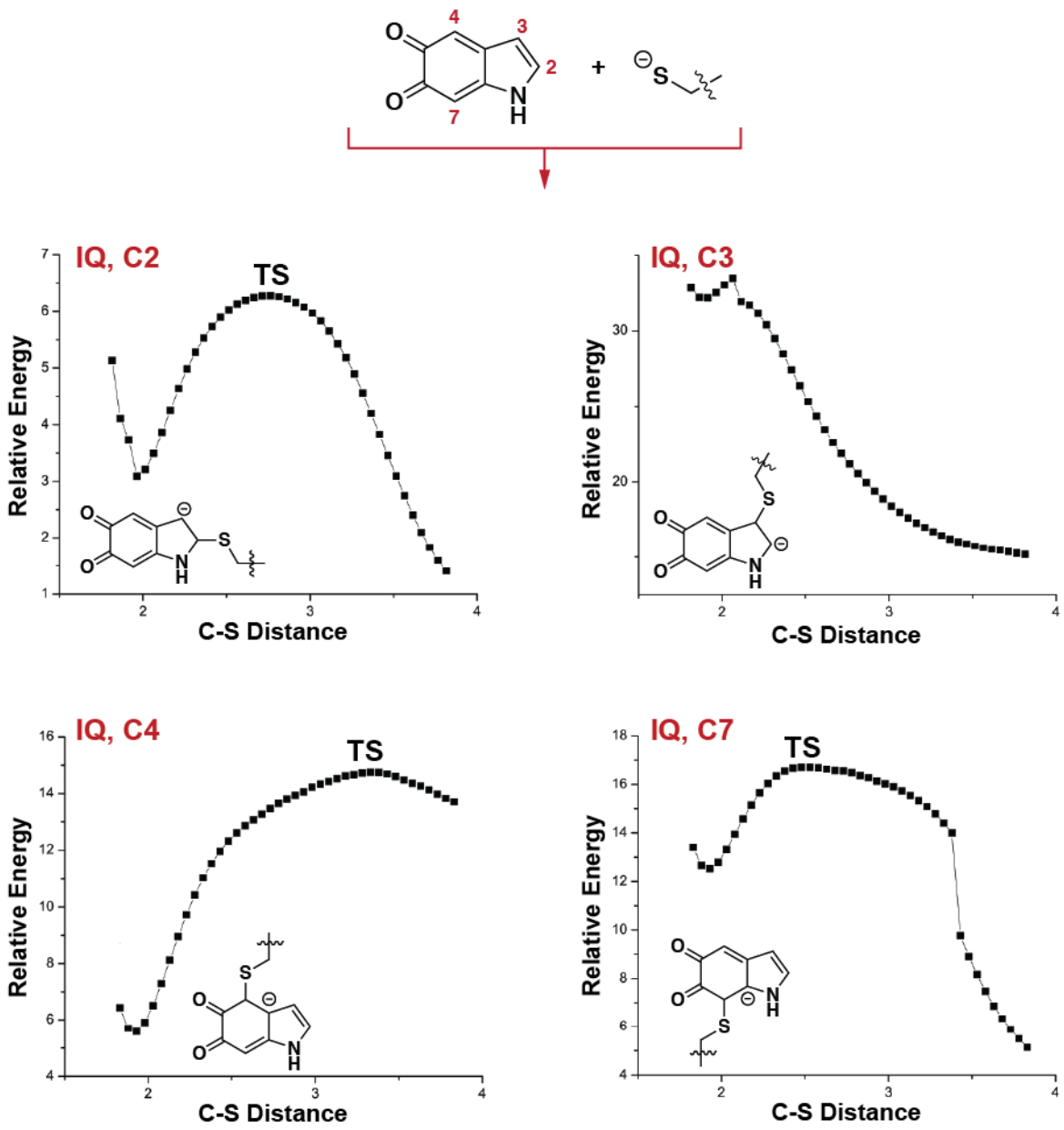

Figure S4. (Related to Figure 4) Potential energy surface for thiolate attack on IQ (indolequinone) at each of four potentially reactive sites (C2, C3, C4, C7). The reactions at positions C2, C4, and C7 exhibit an observable energy barrier, 6.3, 14.7 and 16.7 kcal/mol respectively, suggesting the existence of a stable C-S linked reaction product. The low reaction energy barrier observed for the reaction at C2 suggests reversibility. C-S distances are in Å; relative energies are in kcal/mol; TS = transition state.

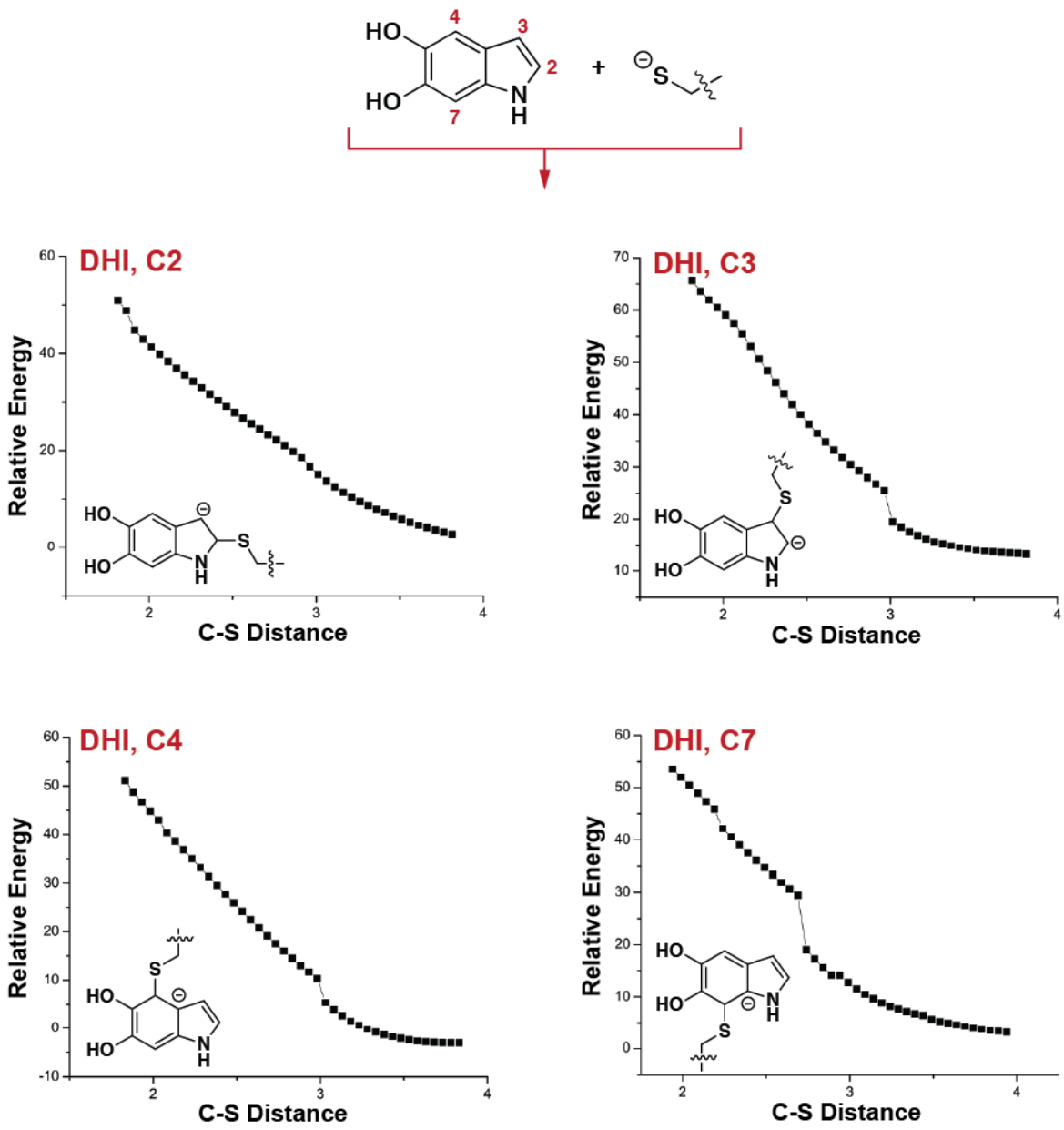

Figure S5. **(Related to Figure 4)** Potential energy surface for thiolate attack on DHI (catechol) at each of four potentially reactive sites (C2, C3, C4, C7). None of these reactions exhibit an energy barrier that would indicate formation of a stable C-S bond at any site. C-S distances are in Å; relative energies are in kcal/mol.

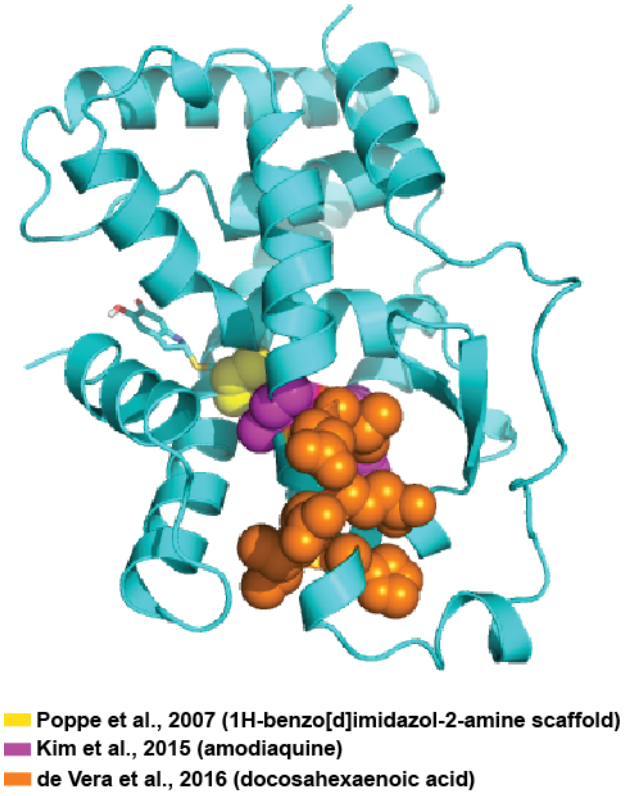

Figure S6. **(Related to Figures 4 and 7)** The DHI/IQ binding site is distinct from the amodiaquine and docosahexaenoic acid binding sites. IQ adduct shown as sticks. Amino acid residues implicated in binding other ligands by NMR spectroscopy are shown as spheres. Poppe et al. identified Cys566 (yellow spheres) as part of the binding site for benzimidazole-like compounds. Kim et al., identified residues (magenta spheres) forming a non-canonical binding site for amodiaquine. de Vera et al., identified residues (orange spheres) forming a canonical binding site for fatty acids.

Table S1. Five cysteine residues within the Nurr1 LBD are conserved across Nurr1 orthologs, Related to Figure 3. Multiple sequence alignment was performed using the Clustal Omega server. Cysteine residues are highlighted in yellow.

```
SP|P43354|NR4A2_HUMAN   RLPSKPKSPQEPSPPSPPVSLISALVRAHVDSNPAMTSLDYSRFQANPDYQMSGDDTQHI 403
SP|Q06219|NR4A2_MOUSE   RLPSKPKSPQDPSPPSPPVSLISALVRAHVDSNPAMTSLDYSRFQANPDYQMSGDDTQHI 403
SP|Q07917|NR4A2_RAT     RLPSKPKSPQDPSPPSPPVSLISALVRAHVDSNPAMTSLDYSRFQANPDYQMSGDDTQHI 403
SP|Q08E53|NR4A2_BOVIN   RLPSKPKSPQEPSPPSPPVSLISALVRAHVDSNPAMTSLDYSRFQANPDYQMSGDDTQHI 403
SP|Q5R5Y4|NR4A2_PONAB   RLPSKPKSPQEPSPPSPPVSLISALVRAHVDSNPAMTSLDYSRFQANPDYQMSGDDTQHI 403
SP|A4IIG7|NR4A2_XENTR   RLPSKPKSPQEPSPPSPPVSLISALVRAHVDSNPAVSSLDYSRFQANPEYQMNGDDTQHI 396
SP|P49869|HR38_DROME    RLPSKPKSPQES-PPSPPISLITALVRSHVDTTPDPSCLDYSHYEEQS-----MSEADKV 878
TR|A9Q8C8|A9Q8C8_DANRE  RLPSKPKSPQESSPPSPPVSLISALVRAHVDSNPSMNSLDYTRFQANPDYQLSGDDTQHI 403
TR|Q6DH08|Q6DH08_DANRE  RLPSKPKSPQDIPVSFTPVNLLNALVRAHIDSNPSMARLDYSKFQTSPEYHSGGDESLHI 398
                         **********:      *:.*:.****:*:*:.*    ***:::: .       .:: ::

SP|P43354|NR4A2_HUMAN   QQFYDLLTGSMEIIRGWAEKIPGFADLPKADQDLLFESAFLELFVLRLAYRSNPVEGKLI 463
SP|Q06219|NR4A2_MOUSE   QQFYDLLTGSMEIIRGWAEKIPGFADLPKADQDLLFESAFLELFVLRLAYRSNPVEGKLI 463
SP|Q07917|NR4A2_RAT     QQFYDLLTGSMEIIRGWAEKIPGFADLPKADQDLLFESAFLELFVLRLAYRSNPVEGKLI 463
SP|Q08E53|NR4A2_BOVIN   QQFYDLLTGSMEIIRGWAEKIPGFTDLPKADQDLLFESAFLELFVLRLAYRSNPVEGKLI 463
SP|Q5R5Y4|NR4A2_PONAB   QQFYDLLTGSMEIIRGWAEKIPGFADLPKADQDLLFESAFLELFVLRLAYRSNPVEGKLI 463
SP|A4IIG7|NR4A2_XENTR   QQFYDLLTGSMEIIRGWAEKIPGFSELHKQDQDLLFESAFLELFVLRLAYRSNPAEGKLI 456
SP|P49869|HR38_DROME    QQFYQLLTSSVDVIKQFAEKIPGYFDLLPEDQELLFQSASLELFVLRLAYRARIDDTKLI 938
TR|A9Q8C8|A9Q8C8_DANRE  QQFYDLLTGSMEIIRGWAEKIPGFTDLPKPDQDLLFESAFLELFVLRLAYRSNPMESKLI 463
TR|Q6DH08|Q6DH08_DANRE  QQFYDLLTASMSIIRGWAEKIPGFTELPKCDQELLFESAFLELFVLRLAYRSNLPEDKLI 458
                         ****:***.*:.:*: :******: :*   **:***:** ***********:.  : ***

SP|P43354|NR4A2_HUMAN   FCNGVVLHRLQCVRGFGEWIDSIVEFSSNLQNMNIDISAFSCIAALAMVTERHGLKEPKR 523
SP|Q06219|NR4A2_MOUSE   FCNGVVLHRLQCVRGFGEWIDSIVEFSSNLQNMNIDISAFSCIAALAMVTERHGLKEPKR 523
SP|Q07917|NR4A2_RAT     FCNGVVLHRLQCVRGFGEWIDSIVEFSSNLQNMNIDISAFSCIAALAMVTERHGLKEPKR 523
SP|Q08E53|NR4A2_BOVIN   FCNGVVLHRLQCVRGFGEWIDSIVEFSSNLQNMNIDISAFSCIAALAMVTERHGLKEPKR 523
SP|Q5R5Y4|NR4A2_PONAB   FCNGVVLHRLQCVRGFGEWIDSIVEFSSNLQNMNIDISAFSCIAALAMVTERHWLKEPKR 523
SP|A4IIG7|NR4A2_XENTR   FCNGVVLNRLQCVRGFGEWIDSIVDFSSNLHSMNIDISAFSCIAALAVITERHGLKEPKR 516
SP|P49869|HR38_DROME    FCNGTVLHRTQCLRSFGEWLNDIMEFSRSLHNLEIDISAFACLCALTLITERHGLREPKK 998
TR|A9Q8C8|A9Q8C8_DANRE  FCNGVVLHRLQCVRGFGEWIDSIVEFSSNLQNMNLDISAFSCIAALAMVTERHGLKEPKR 523
TR|Q6DH08|Q6DH08_DANRE  FCNGMVLHKLQCVRGFGEWIDSIVEFSSNLQSMSLDVSAFSCIAALTIVTERHGLKEPKK 518
                         **** **.: **:*.****::.*::** .*:.:.:*:***:*:.**:::**** *:***:

SP|P43354|NR4A2_HUMAN   VEELQNKIVNCLKDHVTFNNGGLNRPNYLSKLLGKLPELRTLCTQGLQRIFYLKLEDLVP 583
SP|Q06219|NR4A2_MOUSE   VEELQNKIVNCLKDHVTFNNGGLNRPNYLSKLLGKLPELRTLCTQGLQRIFYLKLEDLVP 583
SP|Q07917|NR4A2_RAT     VEELQNKIVNCLKDHVTFNNGGLNRPNYLSKLLGKLPELRTLCTQGLQRIFYLKLEDLVP 583
SP|Q08E53|NR4A2_BOVIN   VEELQNKIVNCLKDHVTFNNGGLNRPNYLSKLLGKLPELRTLCTQGLQRIFYLKLEDLVP 583
SP|Q5R5Y4|NR4A2_PONAB   VEELQNKIVNCLKDHVTFNNGGLNRPNYLSKLLGKLPELRTLCTQGLQRIFYLKLEDLVP 583
SP|A4IIG7|NR4A2_XENTR   VEELQNKIVNCLKDHVTFNNGGLNRPNYLSKLLGKLPELRTLCTQGLQRIFYLKLEDLVP 576
SP|P49869|HR38_DROME    VEQLQMKIIGSLRDHVTYNAEAQKKQHYFSRLLGKLPELRSLSVQGLQRIFYLKLEDLVP 1058
TR|A9Q8C8|A9Q8C8_DANRE  VEDLQNKIVNCLKDQVTFNGGGLNRPNYLSKLLGKLPELRTLCTQGLQRIFYLKLEDLVP 583
TR|Q6DH08|Q6DH08_DANRE  AEELQNKLINCLKDQVSCSG-------ELSKLLEKLPEVRALCTQGLQRIFYLKLEDLVP 571
                         .*:** *:: .*:*:*: .         :*:** ****:*:*..****************

SP|P43354|NR4A2_HUMAN   PPAIIDKLFLDTLPF 598
SP|Q06219|NR4A2_MOUSE   PPAIIDKLFLDTLPF 598
SP|Q07917|NR4A2_RAT     PPAIIDKLFLDTLPF 598
SP|Q08E53|NR4A2_BOVIN   PPAIIDKLFLDTLPF 598
SP|Q5R5Y4|NR4A2_PONAB   PPAIIDKLFLDTLPF 598
SP|A4IIG7|NR4A2_XENTR   PPAIIDKLFLDTLPF 591
SP|P49869|HR38_DROME    APALIENMFVTTLPF 1073
TR|A9Q8C8|A9Q8C8_DANRE  PPAIIDKLFLDTLPF 598
TR|Q6DH08|Q6DH08_DANRE  TPAIIDKLFHDTLPF 586
                         **:*:::*  ****
```

Table S2. (Related to Figure 3) Data collection and refinement statistics.

	Nurr1-DHI/IQ[#]
Wavelength	1.116
Resolution range	40.29 - 3.2 (3.314 - 3.2)
Space group	P 31 2 1
Unit cell	80.586 80.586 225.805 90 90 120
Total reflections	169966 (16629)
Unique reflections	14697 (1414)
Multiplicity	11.6 (11.7)
Completeness (%)	99.58 (99.58)
Mean I/sigma(I)	13.74 (1.22)
Wilson B-factor	98.95
R-merge	0.201 (2.643)
R-meas	0.2103 (2.762)
R-pim	0.06123 (0.7986)
CC1/2	0.999 (0.561)
CC*	1 (0.848)
Reflections used in refinement	14647 (1413)
Reflections used for R-free	1445 (140)
R-work	0.2489 (0.4005)
R-free	0.2954 (0.4024)
CC(work)	0.962 (0.614)
CC(free)	0.901 (0.527)
Number of non-hydrogen atoms	5529
macromolecules	5517
ligands	12
Protein residues	685
RMS(bonds)	0.011
RMS(angles)	1.47
Ramachandran favored (%)	96.05
Ramachandran allowed (%)	3.49
Ramachandran outliers (%)	0.46
Rotamer outliers (%)	0.99
Clashscore	24.39
Average B-factor	120.83
macromolecules	120.85
ligands	111.03
Number of TLS groups	13

[#]Statistics for the highest-resolution shell are shown in parentheses.

Table S3. (Related to Figure 3) Polder map statistics for Cys566-IQ adduct. Only IQ atoms (i.e. no Cys566 atoms) were used in the calculations.

CC(1,2)	0.6288
CC(1,3)	0.7835
CC(2,3)	0.6191
Peak CC(1,2)	0.6465
Peak CC(1,3)	0.7748
Peak CC(2,3)	0.6200

Table S4. (Related to Star Methods) Nurr1 LBD construct names, corresponding protein sequence, and associated experiments.

Construct Name	Protein Sequence
6xHis Tag – TEV Cleavage Site – Nurr1 LBD (Ser-328-598) *Used for x-ray crystallography*	MGSS**HHHHHH**SQDPGSS**ENLYFQS**[328]MVKEVVRTDSLKGRRGRLPS KPKSPQEPSPPSPPV[363]SLISALVRAHVDSNPAMTSLDYSRFQANPDY QMSGDDTQHIQQFYDLLTGSMEIIRGWAEKIPGFADLPKADQDLLFES AFLELFVLRLAYRSNPVEGKLIFCNGVVLHRLQCVRGFGEWIDSIVEFS SNLQNMNIDISAFSCIAALAMVTERHGLKEPKRVEELQNKIVNCLKDHV TFNNGGLNRPNYLSKLLGKLPELRTLCTQGLQRIFYLKLEDLVPPPAIID KLFLDTLPF**
6xHis Tag – Nurr1 LBD (363-598) *Used for thermal shift assays*	MKKG**HHHHHH**GAI[363]SLISALVRAHVDSNPAMTSLDYSRFQANPDYQ MSGDDTQHIQQFYDLLTGSMEIIRGWAEKIPGFADLPKADQDLLFESA FLELFVLRLAYRSNPVEGKLIFCNGVVLHRLQCVRGFGEWIDSIVEFSS NLQNMNIDISAFSCIAALAMVTERHGLKEPKRVEELQNKIVNCLKDHVT FNNGGLNRPNYLSKLLGKLPELRTLCTQGLQRIFYLKLEDLVPPPAIIDK LFLDTLPF**
6xHis Tag – Avi Tag – Nurr1 LBD (363-598) *Used for surface plasmon resonance assays*	MGSS**HHHHHH**SQDPGS**GLNDIFEAQKIEWHE**GSGSG[363]SLISALVRA HVDSNPAMTSLDYSRFQANPDYQMSGDDTQHIQQFYDLLTGSMEIIR GWAEKIPGFADLPKADQDLLFESAFLELFVLRLAYRSNPVEGKLIFCNG VVLHRLQCVRGFGEWIDSIVEFSSNLQNMNIDISAFSCIAALAMVTERH GLKEPKRVEELQNKIVNCLKDHVTFNNGGLNRPNYLSKLLGKLPELRT LCTQGLQRIFYLKLEDLVPPPAIIDKLFLDTLPF**

Bolded sequences: 6xHis Tag (HHHHHH); TEV recognition sequence (ENLYFQS); BirA biotinylation recognition sequence (GLNDIFEAQKIEWHE).

Table S5. (Related to Star Methods) Primers used for qPCR.

Gene name	Gene ID number	Forward Primer	Reverse Primer
nurr1 (NR4A2)	NM_001113484.1	CAGGTCCAACCCGATGGAAA	TCCGTGTCTCTCTGTGACCA
th	NM_131149.1	GCTCTCAGCACGCGATTTTT	ATGGACGCAATCCGGTTCAG
vmat2 (slc18a2)	NM_001256225.2	TCTTCTGTGGCAGGTATGGG	CCTCCCAGTGCAATCCCAAT
dat (slc6a3)	NM_131755.1	TGCTACAAGAATGGCGGAGG	GTAGGAGCCCACATACAGCG
ddc (addc)	NM_213342.1	CAAAGGAGGTGGGGTCATCC	CACCGATGAGTGTGCCTGAT
elf1α	NM_131263.1	TTCTCAGGCTGACTGTGC	CCGCTAGCATTACCCTCC